

Central European Journal of Chemistry

A prospect for LiBH₄ as on-board hydrogen storage

Review Article

Ivan Saldan*

Helmholtz-Zentrum Geesthacht, Institute of Materials Research, Geesthacht 21502, Germany

Received 16 December 2010; Accepted 16 May 2011

Abstract: In contrast to the traditional metal hydrides, in which hydrogen storage involves the reversible hydrogen entering/exiting of the host hydride lattice, LiBH₄ releases hydrogen *via* decomposition that produces segregated LiH and amorphous B phases. This is obviously the reason why lithium borohydride applications in fuel cells so far meet only one requirement – high hydrogen storage capacity. Nevertheless, its thermodynamics and kinetics studies are very active today and efficient ways to meet fuel cell requirements might be done through lowering the temperature for hydrogenation/dehydrogenation and suitable catalyst. Some improvements are expected to enable LiBH₄ to be used in on-board hydrogen storage.

Keywords: LiBH₄ • Hydrogen storage capacity • Thermodynamics • Kinetics © Versita Sp. z o.o.

1. Introduction

Hydrogen has potential to be one of the alternative energy carriers, which should replace traditional fossil fuels in the near future. The direct production of this new fuel would be made by electrolysis of water and under combustion of hydrogen only water will have been obtained, too. The hydrogen energy content is equal to 142 MJ kg⁻¹, which is much larger than petroleum – about 47 MJ kg-1. Therefore the hydrogen chemical energy would be feasible to use for combustion engines and fuel cells. A modern, commercially available car with a range of 400 km burns about 24 kg of petrol in a combustion engine; to cover the same range, 8 kg hydrogen are needed for the combustion engine version or only 4 kg hydrogen for an electric car with a fuel cell. But one of the most discouraging challenges for widespread use of hydrogen as a fuel is the absence of a commercially viable hydrogen storage technology. Only a hydrogen storage material with ~9 wt.% H₂ gravimetric and ~80 kg H₂ m⁻³ volumetric density in fuel cell can replace petroleum fuel in vehicles on a large scale [1].

In this paper the current state and future outlook on the thermodynamics and kinetics of $LiBH_4$ as a reversible hydrogen storage material adapted to the fuel cell application have been reviewed.

2. Theoretical predictions to meet fuel cell requirements

Although progress is being made in fuel cell technology, a viable method of on-board hydrogen storage is still under investigation. In order to have the advantages of petrol and diesel, hydrogen storage materials should operate at temperatures 243–323 K with fast (<5 min) reversibility (~90%) during at least 500 cycles [2]. From a thermodynamic standpoint, reversible decomposition of LiBH₄ at moderate conditions (P(H₂) ≤100 bar; T ~300 K) is equivalent to a reaction enthalpy around ~25–35 kJ mol⁻¹ H₂. Therefore the development of different methods to adjust hydrogen storage materials to have suitable thermodynamic properties is very crucial.

2.1 Thermal decomposition of LiBH,

Complex hydrides, including light metal (Li), have sufficient gravimetric hydrogen storage capacity which is suitable for fuel cell vehicles. This is the main reason why lithium complex hydrides such as ${\rm LiNH_2}$ (with ~8.8 wt.% ${\rm H_2})$ and ${\rm LiBH_4}$ (with ~18.5 wt.% ${\rm H_2})$ are being studied by many research groups. Particularly, the latter can desorb theoretically about ~13.5 wt.% ${\rm H_2}$ by reaction (1), because LiH is too stabile (up to 1173 K [3,4]):

^{*} E-mail: ivan_saldan@yahoo.com

$$LiBH_4 \rightarrow LiH + B + \frac{3}{2}H_2 \tag{1}$$

The experimental value of enthalpy for this reaction is about \sim 68.6 kJ mol⁻¹ H₂, therefore the temperature for hydrogen release is close to \sim 680 K [5]. The thermal desorption of LiBH₄ shows us a structural transition around \sim 380 K and melting point at \sim 550 K.

The precise theoretical observation of the LiBH, stability at absolute zero temperature as well as its most possible intermediates at heat treatment are discussed in [6]. Based on the existence of alkali-metal B-H inorganic compounds it was assumed that LiB₃H₈, LiB₆H₆ and LiB₁₂H₁₂ should have the same crystal structure as CsB₃H₈ [7], K₂B₆H₆ [8] and K₂B₁₂H₁₂ [9], respectively. The stability of all possible intermediates such as Li₂B₂H₂ (5≤n≤12) was predicted using firstprinciples calculations. The output compounds had different symmetry depending on the structure of [B H] clusters. Moreover the theoretical results indicated the cubic and monoclinic types of structure for Li₂B₄₂H₄₂ and based on cohesive energy value, which was larger for the last, only Li₂B₁₂H₁₂ with P2₁/n structure was considered as a possible intermediate. The calculated enthalpy of LiBH, formation (with orthorhombic Pnma symmetry; with zero-point energy correction) was equal to -56 kJ mol⁻¹ H₂ [10]. And only Li₂B_nH_n (10≤n≤12) compounds showed more negative values: -87; -79; $-125 \text{ kJ mol}^{-1} \text{ H}_2 \text{ for } \text{Li}_2 \text{B}_{10} \text{H}_{10}; \text{Li}_2 \text{B}_{11} \text{H}_{11}; \text{Li}_2 \text{B}_{12} \text{H}_{12},$ respectively [6]. Taking into account the relationship between the formation enthalpy and the mole fraction of H2 the authors concluded that the most possible intermediates for LiBH₄ decomposition should be LiB₁₂H₁₂ and the total hydrogenation/dehydrogenation process for lithium borohydrides can be written as follows:

$$\begin{array}{c} {\sf LiBH_4} \leftrightarrow \frac{1}{12} {\sf Li_2B_{12}H_{12}} + \frac{5}{6} \, {\sf LiH} + \frac{13}{12} {\sf H_2} \leftrightarrow \\ \leftrightarrow {\sf LiH} + {\sf B} + \frac{3}{2} {\sf H_2} \end{array} \tag{2}$$

In this case the calculated enthalpy (without zeropoint energy correction) and hydrogen content for the first and second steps were 56 kJ mol⁻¹ H_2 & ~10 wt.% H_2 and 125 kJ mol⁻¹ H_2 & ~4 wt.% H_2 , correspondently. The most interesting result was that the calculated enthalpy for the first step in process (2) is lower than that for the direct hydride removal reaction (1). These theoretical calculations on the energy of monoclinic $\text{Li}_2\text{B}_{12}H_{12}$ provided the upper-limit value for thermodynamic stability. Moreover, it was predicted by phonon density of states that bending modes for $\text{Li}_2\text{B}_{12}H_{12}$ with $P2\sqrt{n}$ structure have lower frequencies than those of LiBH_4 (Pnma). Lithium borohydride desorbs hydrogen at temperatures above the melting point. The latent heat of fusion is 0.078 eV per formula unit [11] and similar values

were expected for $\text{Li}_2\text{B}_n\text{H}_n$. Among the all considered closo-type dianions the $[\text{B}_{12}\text{H}_{12}]^{2-}$ was the most stable:

$$n B + \frac{n}{2}H_2 + 2 e^{-} \leftrightarrow [B_n H_n]^{2-}$$
 (3)

This means that Li₂B₁₂H₁₂ should be present during the hydrogenation/dehydrogenation process for LiBH₄ as an intermediate phase.

Because of the fact that B_2H_6 can be released during the desorption of borohydrides [12], another reaction mechanism for the rehydrogenation of LiBH₄ was proposed in [13]:

It is possible that hydrogen desorption and absorption can occur for lithium borohydride at low temperature and pressure by using an intermediate compound.

In recent work [14] LiBH, decomposition was studied by synchrotron radiation powder X-ray diffraction (SR-PXD) and solid state CP/MAS NMR at variable temperature. The experimental results showed evidence of the presence of three new phases, which were not similar to those theoretically predicted in [6]. Two phases are denoted as I and II, they were formed by partial dehydrogenation with slightly lower hydrogen content than stoichiometric LiBH₄. This observation was explained by the similar Li and B coordination in phases I and II to that in LiBH₄. But the limited SR-PXD data has not yet allowed a complete structural analysis for neither phase I nor II. Boron NMR revealed a minor signal at $\delta(^{11}B) \approx -3.5$ ppm (0.3%) that was suggested to another phase existence; most probably it was a complex between water and LiBH, or alternatively, was an impurity that was not identified by SR-PXD.

In experimental work [15] the thermodynamic parameters for reaction (1) were precisely determined by the van't Hoff equation: $\Delta H = 74$ kJ mol⁻¹ H_2 and $\Delta S = 115$ J K⁻¹ mol H_2 . This means that the decomposition temperature (T_d) for LiBH $_4$ at 1 bar hydrogen pressure can be 643 K. These thermodynamic properties obviously are not appropriate for general criteria under fuel cell applications. Moreover, the reversibility for reaction (1) together with very slow kinetics should be improved as well.

2.2 Partial cation substitution in LiBH,

Recent experiments suggest that the tetragonal configuration of BH₄ complexes is strongly distorted [10]. Analyses for the electronic structure and the Born effective charge tensors indicated that Li atoms are ionized as Li⁺ cations. Aboron atom constructs *sp*³ hybrids

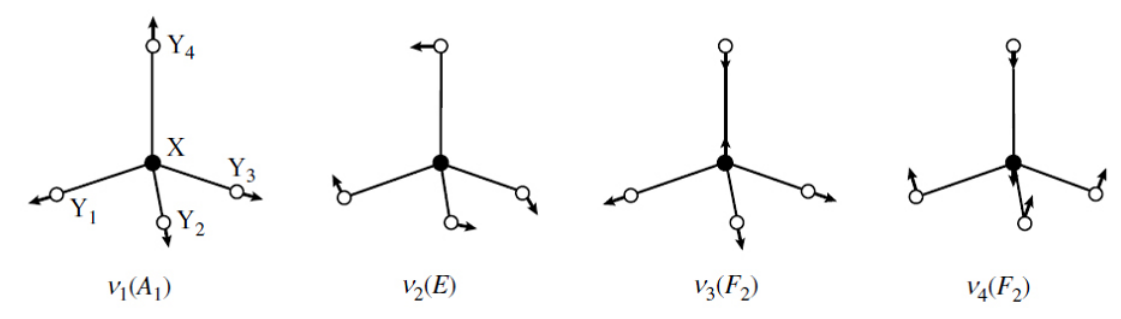


Figure 1. Schema of atomistic vibrations in XY₄ group; X is B atom, Y is H atom.

and forms covalent bonds with surrounding H atoms. The Γ -phonon frequencies originated from the internal B-H bending and stretching vibrations of BH $_4$ complexes reproduced by the molecular approximation, suggesting strong bonding of BH $_4$. These bonding properties are expected to be held even at high temperature but in another structure – hexagonal P6 $_3$ mc. It was proposed that a charge compensation by Li $^+$ cation would be a key feature for the stability of the internal bonding of [BH $_4$]-anions. Therefore a suppression of the charge transfer by the partial substitution Li atoms by other light metals would be effective to decrease thermodynamic stability of whole LiBH $_4$ compound.

First, the correlation between B-H atomistic vibrations in the [BH₄]- anion and melting temperatures (T_m) of MBH₄ (M=Li, Na, K) were clarified in [16]. Stretching modes of the modes of B–H bonds (v_1 and v_3) are due to changes in the distance between the B and H atoms; the bending modes (v_2 and v_4) – the change in the angles between the H-B-H bonds (Fig. 1). On the one hand, the Raman shifts of the bending mode v_2 decrease in of the following order: LiBH₄ > NaBH₄ > KBH₄ > RbBH₄ > CsBH₄; on the other hand, the Raman shifts of the stretching mode v_1 decrease in the order of NaBH₄ > KBH₄ > RbBH₄ > CsBH₄. The smaller value of the stretching mode and related spectra at around 2200-2400 cm⁻¹ of LiBH₄ comparing to those of NaBH₄ and KBH₄ should be due to the less-density orthorhombic structure [17] that is different with respect to crystal structure of NaBH, and $KBH_{A}(Fm3m)$. A linear relationship is expected between earth metals and the atomistic vibration of [BH₄]- anions in their corresponding borohydrides. Obviously metals of the first group in Periodic Table have the same type of influence on [BH₄]- anions but only with a difference in the value.

The differential scanning calorimetry (DSC) profiles of MBH₄ (M = Li, Na, K) during heating up to 900 K under 1 bar hydrogen pressure has been previously reported in [16]. Taking into account endothermic peaks only for melting reaction (the structural transformation took place at ~380 K for LiBH₄; ~10 K for NaBH₄;

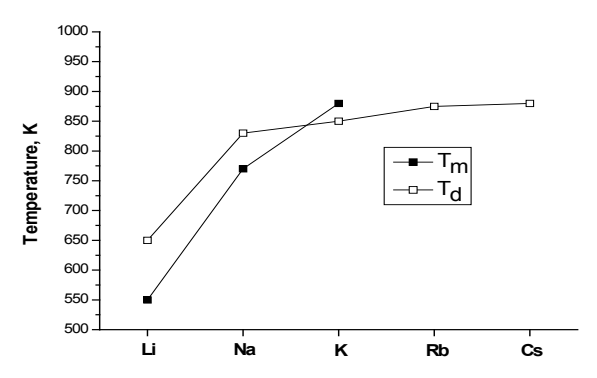


Figure 2. Dependence of melting and decomposition temperatures (T_m and T_d, respectively) for MBH₄ (M = Li; Na; K; Rb; Cs) compounds.

and ~1.5 K for KBH $_4$), one can conclude that melting temperature (T_m) increases in of the following order: LiBH $_4$ < NaBH $_4$ < KBH $_4$ (Fig. 2). Similar behavior is present also for T_d . Because of the decrease in stretching modes v_1 and bending modes v_2 (except for LiBH $_4$ because of structure) and the increase of T_m and T_d in the order LiBH $_4$; NaBH $_4$; KBH $_4$; RbBH $_4$; CsBH $_4$, it can be concluded that smaller cation size or higher valence cation with larger electronegativity would be preferred for lower T_d of MBH $_4$ compounds. Behavior of the curves (Fig. 2) can be explained by a small change in cell parameters of borohydrides as a total result of different influences between cations and anions in polarized molecules.

In recent work [18], a correlation between the T_d and the Pauling electronegativity (χ_p) was observed experimentally for $M(BH_4)_n$, where M was rare-earth and transition metal. Moreover, a good correlation between estimated enthalpy for $M(BH_4)_n$ decomposition and the observed T_d , was presented as confirmation to predict the stability of borohydrides. In other words, the thermodynamic stability of LiBH $_4$ can be reduced by partial substitution of Li on another light element with less metallic in nature and subsequently the B-H bonds may be weakened and T_d should be decreased.

But today there is only a handful of experimental data on partial cation substituted LiBH₄ (LiK(BH₄)₂ [18-22] and LiSc(BH₄)₄ [22]) which shows that partial substitution of

Li by another element from 1a group in Periodic Table could not decrease T_d . Therefore it is expected that reduction of T_d could be for cation substituted LiBH $_4$ by transition elements although hydrogen gravimetric capacity of this new compound will be also reduced [23].

2.3 Partial H-atom substitution inside [BH₄]⁻

Since H and F atoms are very similar in size and valence, H→F substitution inside BH, tetrahedron may be possible. And these compounds, called "hydridofluorides", in most cases have the same crystal structure as their corresponding hydrides. Moreover, thermodynamic properties can be changed gradually by progressive H→F substitution. The direct reaction of hydrogen on a mixture of Na with Mg or NaF with Mg resulted in the synthesis of orthorhombic NaMgH_a and NaMgH,F, respectively [24]. Another example was Na₃AlH₂F₄ made from NaF and Al in the presence of TiF₃ [25]. For NaMgH_{3-x}F_x compounds their enthalpy of formation increases with increasing x value [26]; but in the case of Na₁₂Al₄H_{24-x}F_x – results in gradually enthalpy reducing. A change in ΔH from LiBH, to LiBF, would be interesting to observe too.

In recent work [27], the decomposition reaction of LiBH, with F anion doping was investigated by firstprinciples calculations. The computed cell parameters of LiBH, were in good agreement with the experimental data (space group Pnma, a=57.17858(4), b=54.43686(2), c=56.80321(4) Å [28]). According to the calculation H→F, substitution can be possible for LiBH, at its formation (as LiBH, F,) and under its decomposition for LiH (as LiH, F,). A 1×2×1 LiBH, supercell consisting of 48 atoms (LigBgHgg), a 1×2×1 LiH supercell containing 16 atoms (Li_sH_s), and a crystallographic unit cell containing 12 atoms to represent α-boron were constructed to study LiBH, decomposition. Five possible theoretical reactions under decomposition of Li_gB_gH₃₂,F_g (x= 1-4), including persisting its substitutional feature in LiH lattice, combining with Li cation to generate segregated LiF phase, combining with B to generate gaseous BF3, bonding with H to generate gaseous HF, or forming gaseous F2 by coupling with another F, were presented:

$$\text{Li}_{8}\text{B}_{8}\text{H}_{32-x}\text{F}_{x} \rightarrow \text{Li}_{8}\text{H}_{8-x}\text{F}_{x} + 8 \text{ B} + 12 \text{ H}_{2}$$
 (5)

$$\text{Li}_{8}\text{B}_{8}\text{H}_{32-x}\text{F}_{x} \rightarrow \text{Li}_{8-x}\text{H}_{8-x} + \text{Li}_{x}\text{F}_{x} + 8 \text{ B} + 12 \text{ H}_{2}$$
 (6)

$$\text{Li}_{8}\text{B}_{8}\text{H}_{32-x}\text{F}_{x} \rightarrow \text{Li}_{8}\text{H}_{8} + \text{x/3 BF}_{3} + (8-\text{x/3}) \text{ B} + (12-\text{x/2}) \text{ H}_{2}$$
 (7)

$$\text{Li}_{8}\text{B}_{8}\text{H}_{32-x}\text{F}_{x} \rightarrow \text{Li}_{8}\text{H}_{8} + \text{H}_{x}\text{F}_{x} + 8\text{B} + (12-x)\text{H}_{2}$$
 (8)

$$\text{Li}_{8}\text{B}_{8}\text{H}_{32-x}\text{F}_{x} \rightarrow \text{Li}_{8}\text{H}_{8} + 8\text{B} + x/2\text{ F}_{2} + (12-x/2)\text{ H}_{2}\text{ b}$$
 (9)

In Fig. 3, the calculated decomposition enthalpy of $\text{Li}_{8}\text{B}_{8}\text{H}_{32-x}\text{F}_{x}$ (x = 1–4) depending on H \rightarrow F substitution is demonstrated. According to the calculation, reactions (5) and (6) are more favorable than others. It means that the possibility of the generation of gaseous fluorine phases (BF₃; HF; F₂) at Li₈B₈H_{32-x}F_x (x = 1-4) decomposition should be excluded. The tendency of reaction enthalpy decreasing with H→F substitution increasing for reaction (5) can be explained by F substitution in both $\text{Li}_{8}\text{B}_{8}\text{H}_{32-x}\text{F}_{x}$ and $\text{Li}_{8}\text{H}_{8-x}\text{F}_{x}$. The formation enthalpies of these F-substituted hydrides are much more negative than those of the pure counterparts, but with an absolute decrease in Li,H, F, larger than that in Li,B,H,, F. The value of enthalpy decomposition for LiBH, with and without zero-point energy corrections were 60.9 and 77.7 kJ mol H₂, respectively, which are in a good agreements with those reported in [3-5,10,15].

In order to model solid solutions between LiBH₄ and LiBF₄, the adopted procedure in [29] contemplated the following steps: (i) classification, by symmetry equivalence, of all the possible configurations obtained at the same F content; (ii) full geometry optimization, to compute vibrational and thermodynamic properties of the Li–B–H–F structures; (iii) calculation of Δ H, Δ S and Δ G at T = 298 K and P = 0.1013250 MPa for the reaction:

$$(1-a/16) \text{ LiBH}_4 + (a/16) \text{ LiBF}_4 \rightarrow (1/4) \text{ Li}_4 \text{B}_4 \text{H}_{16-a} \text{F}_a$$
 (10)

Value a showed the number of F ions which can substitute H inside the unit cell $(0 \le a \le 16)$.

The quantum-mechanical data of mixed compounds were used to derive the ΔH curve (Fig. 4) by thermodynamic modeling according to the equation:

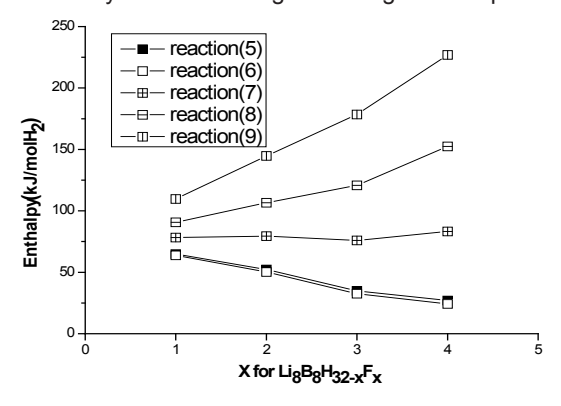


Figure 3. Calculated decomposition enthalpy of $Li_8B_8H_{32-x}F_x$ (x = 1-4) at the reactions (5-9).

$$\Delta H_{\text{mix}} = x(1 - x)[L_0 + L_1(2x - 1)] \tag{11}$$

Value x is the molar fraction of LiBF $_4$ and L $_0$ = 62438 J mol $^{-1}$ and L $_1$ = - 9750 J mol $^{-1}$ were the interaction parameters.

The main conclusion of this theoretical calculation was that at room temperature changes in enthalpy for all compositions from the pure hydride to the pure fluoride were positive. This indicates no formation of mixed ${\rm LiBH_4-LiBF_4}$ compounds at room temperature and 1 bar of pressure.

In experimental work [30], only LiBH $_4$ and MgF $_2$ have been found as the main products of mechanochemical interactions between LiF and MgB $_2$. Nevertheless in this work NEXAFS data is the next hint of LiBH $_{4-x}$ F $_x$ existence after ATR–FTIR observations in [31] for LiF–MgB $_2$ system. In the next studies possible fluorine substitution for hydrogen atom inside [BH $_4$] $^-$ anion will be proposed by another experimental methods (e.g. wet chemical). Similar [BH $_4$] $^-$ anion modification have been already experimentally confirmed for [BH $_3$ OH] $^-$, [BH $_3$ OR] $^-$ and [BH $_3$ NH $_4$] $^-$ in [32], [33] and [34], respectively.

2.4 Reactive hydride composites based on LiBH,

In principle, two or more hydrides can chemically react with each other if the total heat of the mixture formation has an exothermic effect. And the value of the mixture reaction enthalpy can be altered by selecting certain hydride-reagents. The method produces a new composite known as "Reactive Hydride Composite" (RHC). If it is thermodynamically possible to create a mixture of LiBH $_{\!_{4}}$ with another light hydride to decrease its T $_{\!_{d}}$ and at the same time remain the high hydrogen content, it can be one of the solutions to obtain appropriate reversible hydrogen storage material in fuel cells.

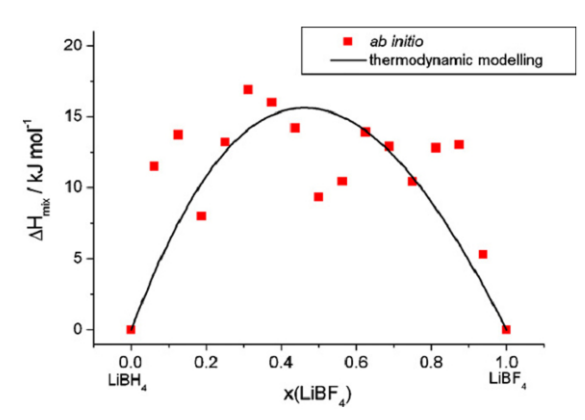


Figure 4. Calculated excess enthalpy of mixing as a function of composition in the orthorhombic LiBH₄-LiBF₄ solid solution at 298 K and 1 bar (line) in comparison with the results from first-principles calculations (squares).

One of the most noticeable RHC examples is the mixture of $LiBH_4$ with MgH_2 experimentally studied in [35]:

$$LiBH_4 + \frac{1}{2}MgH_2 \rightarrow LiH + \frac{1}{2}MgB_2 + 2H_2$$
 (12)

This reaction (12) yielded maximum ~11.5 wt.% H_2 and reversibly – more than 9 wt.% H_2 . Thermodynamical properties were estimated by the van't Hoff equation: $\Delta H = 40.5 \text{ kJ mol}^{-1} H_2$ and $\Delta S = 81.3 \text{ J K}^{-1} \text{ mol } H_2$. These data show that reaction (12) can be carried out at 498 K temperature under 1 bar hydrogen pressure. Because the equilibrium pressure for Mg H_2 /Mg system is higher than for the RHC at above 633 K it means that reaction (12) should be changed to another one as follows:

$$LiBH_4 + \frac{1}{2}Mg \rightarrow LiH + \frac{1}{2}MgB_2 + \frac{3}{2}H_2$$
 (13)

It is known that hydrogenation of Mg is exothermic, therefore, the enthalpy for reaction (13) is expected to be less than for reaction (12).

Other possible reactions with these light hydrides were predicted in recent theoretical work [36]:

$$4 \text{ LiBH}_4 + \text{MgH}_2 \rightarrow 4 \text{ LiH} + \text{MgB}_4 + 7 \text{ H}_2$$
 (14)

7 LiBH₄ + MgH₂
$$\rightarrow$$
 7 LiH + MgB₇ + $\frac{23}{2}$ H₂ (15)

The calculated enthalpy by DFT for reactions (14) and (15) were 53.5 kJ mol⁻¹ H_2 and 55.1 kJ mol⁻¹ H_2 , respectively. But any experimental results were not obtained for these reactions which can yield a maximum of ~12.5 wt.% H_2 and ~13 wt.% H_2 at completion for (14) and (15), respectively. Another example of HRC with similar expectations is a mixture of LiBH₄ and CaH₅:

$$6 \operatorname{LiBH}_{4} + \operatorname{CaH}_{2} \to 6 \operatorname{LiH} + \operatorname{CaB}_{6} + 10 \operatorname{H}_{2} \tag{16}$$

The DFT calculation estimated reaction (16) with a possible enthalpy of 47.0 kJ mol $^{-1}$ H $_2$ and maximum theoretical capacity \sim 12 wt.% H $_2$. The mixture LiBH $_4$ with LiNH $_2$ experimentally can produce hydrogen up to \sim 7.8 wt.% H $_2$ at 522 K under 1 bar hydrogen pressure [37,38]:

$$LiBH4 + 2 LiNH2 \rightarrow Li3BN2 + 4 H2$$
 (17)

The calculated reaction enthalpy was 24 kJ mol⁻¹ H_2 and theoretically 11.9 wt.% H_2 was predicted [36]. But in reality, under heating this composite forms quaternary hydride ($Li_4BN_3H_{10}$; space group $I2_13$; cell parameter a = 10.679(1)-10.672(1) Å [39]) as intermediate phase

which decomposes at room temperature. This is why the phase composition of the RHC is very sensitive to ambient conditions.

Hydrides of transition metals demonstrate lower gravimetric density of hydrogen with respect to light metal hydrides. Nevertheless, from a thermodynamic standpoint, it is interesting to predict possibilities of new RHC based on LiBH $_4$ with at least ScH $_2$ and TiH $_2$. The DFT calculations in [36] gave some reactions which are worth of our attention:

$$LiBH_4 + \frac{1}{2}ScH_2 \rightarrow LiH + \frac{1}{2}ScB_2 + 2H_2$$
 (18)

The theoretical results showed that reaction (18) can release \sim 8.9 wt.% H_2 on completion and their calculated reaction enthalpy should be 34.7 kJ mol⁻¹ H_2 . A similar reaction can be possible with TiH₂:

$$LiBH_4 + \frac{1}{2}TiH_2 \rightarrow LiH + \frac{1}{2}TiB_2 + 2H_2$$
 (19)

DFT calculations indicated 6.5 kJ $\rm mol^{-1}~H_2$ and the theoretical maximum hydrogen content can be only ~8.7 wt.% $\rm H_2$.

It is no surprise that the mixtures LiBH₄ with transition metals hydrides give lower hydrogen gravimetric density, although their thermodynamic data are not worse in regards to the mixture of LiBH₄ with light metal hydrides. Since all above mentioned reactions were observed only theoretically, their experimental examination would be useful to get answers as to how much hydrogen can be loaded/unloaded for these new RHCs at moderate conditions.

2.5 Carboninfluence on LiBH₄ dehydrogenation/rehydrogenation

It is known that carbon can react with hydrogen to produce hydrocarbons. But every allotropic carbon modification with its own specific structure should have different thermodynamics for reaction with hydrogen. Graphite is expected to be more difficult to react with hydrogen than activated carbon or carbon black. Nevertheless, graphite in nano-scale as nanofibers and Li-, K-intercalated graphite were studied with regards to hydrogen storage materials [40,41]. Theoretically graphite can store hydrogen at 65 meV/H₃ through the dramatic swelling of interlayer separation, where one hydrogen molecule can be placed on the top of every graphite hexagon (~7.7wt.% H₂). But hydrogen intercalation causes a big interlayer relaxation (in ~1.70 times), therefore, the optimal H₂ adsorption distance is far too large for energetically favorable adsorption of a hydrogen molecule between two graphene sheets inside graphite [40]. In order to increase the possibility of graphite interaction with hydrogen, the alkali-doping of graphite nanofibers was introduced in some recent works [41,42]. Calculations showed stronger hydrogen adsorption on Li-intercalated graphite with respect to K-one. Only physical adsorption had been located, the binding energy of which is higher at 0 K and become near zero relatively at 298 K. Thus un-cyclable hydrogen is actually not adsorbed on alkali atoms but only on defects of graphite, or so-called "carbon edge sites", where hydrogen adsorption is thermodynamically very favorable [41]. These defects were produced by the repeated heat treatment at 523 K for 12 h [42]. After absorption/desorption cycling for both Li- and K-doped graphite nano-fibers, H2O impurity was present at thermogravimetry and it could be the reason why no hydrogen adsorption was observed for Li-doped graphite. But for K-doped graphite only 1.3 wt.% H_a was achieved near at room temperature. It should be dissociatively adsorbed hydrogen, or in other words, chemically adsorbed hydrogen, because thermodynamically it is very difficult to desorb hydrogen atoms from these carbon edge sites.

Using DFT calculations in [36] for LiBH $_4$ mixtures with carbon in solid phase non-hydrocarbon species the enthalpy value ~31.8 kJ mol 1 H $_2$ with a hydrogen capacity of ~12 wt.% H $_2$ at completion can be achieved by the reaction:

$$LiBH_4 + C \rightarrow LiBC + 2 H_2$$
 (20)

In practice, carbon nano-tubes (C_{nano}) , where used to check this reaction [43]. No CH, was detected by mass spectroscopy during hydrogenation/dehydrogenation of LiBH₄ mixtures with C_{nano} (Shenzen Nanotech Port Co., Ltd., China). System LiBH₄/C_{nano}, where C_{nano} was introduced as multi-wall carbon nanotubes (MWCNTs) was expected to show better thermodynamic properties with respect to RHCs. In this experimental work, LiBH₄/ C_{nano} with different mass ratios (2:1; 1:1 and 1:2) were mechanically milled under inert gas for 1 h. For all mixtures, the thermogravimetry showed that the initial temperature for hydrogen desorption was ~520 K and the main temperature peaks were ~733 K; ~648 K and ~633 K for 2:1; 1:1 and 1:2 LiBH₄/C_{nano} mixtures, respectively. The hydrogen storage capacity was: ~11; ~8.55 and ~6 wt.% H₂ for the same direction of the mixtures. The 1:2 mass ration LiBH₄/C_{nano} mixture was partly rehydrogenated at 673 K under 100 bar hydrogen pressure and the main hydrogen desorption peak was on 10 K lower than for the first desorption though hydrogen release was only 1.26 wt.% H₂. XRD analysis of 1:2 mass ratio LiBH₄/C_{nano} mixture showed LiBH₄ and C; Li₂C₂, C and LiOH; Li₂C₂, C and LiH for milled, dehydrogenated and rehydrogenated samples, respectively. Therefore, the reaction paths were proposed as follows:

$$\begin{aligned} \text{LiBH}_{4} + \text{C} &\rightarrow \frac{1}{2} \text{Li}_{2} \text{C}_{2} + \text{B} + 2 \text{ H}_{2} \rightarrow \\ &\rightarrow \text{LiH} + \text{C} + \text{B} + \frac{3}{2} \text{ H}_{2} \end{aligned} \tag{21}$$

Carbon in the form of non-hydrocarbon species is expected to moderate thermodynamics for LiBH $_4$ decomposition/formation by reaction (20) although the reaction paths are not determined yet. The influence of carbon on LiBH $_4$ reversible decomposition is visible, but neither graphite nano-fibers nor MWCNTs can react directly with hydrogen.

From a thermodynamic standpoint, these carbon species can be involved even in the RHC reactions and some of them have been calculated by DFT in [36]. Reaction (12) theoretically can be performed more easily when 1 mol of carbon would be added:

$$LiBH_4 + \frac{1}{2}MgH_2 + C \rightarrow \frac{1}{2}MgB_2C_2 + LiH + 2H_2$$
 (22)

Calculations had given 39.9 kJ mol^{-1} H₂ of reaction enthalpy and 8.6 wt.% H₂ of maximum gravimetric density. This enthalpy value is better than for reaction (12) although hydrogen storage capacity is gone out of the necessary limit. The next similar example could be reaction with CaH₂:

$$LiBH_4 + \frac{1}{2}CaH_2 + C \rightarrow \frac{1}{2}CaB_2C_2 + LiH + 2H_2$$
 (23)

The reaction is thermodynamically feasible and even in comparison with reaction (16) the calculated enthalpy is lower (~45.9 kJ mol $^{-1}$ H $_{\!_2}$). But again theoretical gravimetric density is also decreased (7.3 wt.% H $_{\!_2}$). In the end, two possible reactions involving ScH $_{\!_2}$ were predicted as thermodynamically very interesting:

$$LiBH_4 + \frac{1}{2}ScH_2 + \frac{1}{2}C \rightarrow \frac{1}{2}ScB_2C + LiH + 2H_2$$
 (24)

$$LiBH_4 + \frac{1}{2}ScH_2 + C \rightarrow \frac{1}{2}ScB_2C_2 + LiH + 2H_2$$
 (25)

Because of increasing RCHs weight on carbon mass the total hydrogen storage capacity is decreased to 7.9 wt.% $\rm H_2$ and 7.0 wt.% $\rm H_2$, but the calculated values of enthalpy are quite good – 37.6 kJ mol⁻¹ $\rm H_2$ and 36.9 kJ mol⁻¹ $\rm H_2$ for (24) and (25), respectively. Comparing $\Delta \rm H$ values for these reactions together with that of (18) it can be concluded that all reaction enthalpies are very close to each other. This a priori means that the carbon modifications show more obvious catalytic effects on RHCs mixtures.

2.6 Promising approaches and reactions of LiBH₄ with regards to fuel cell applications

From all above mentioned chapters the main approaches to meet fuel cell applications of LiBH₄ can be combined as follows:

- (i) For thermodynamically stable LiBH₄ the partial substitution of Li⁺ on less ionized metallic atoms can be a good example to destabilize interactions between cations and anions. However, it is expected to decrease the hydrogen storage capacity.
- (ii) Because of the low weight of F-atoms and the theoretically observed influence on $\text{Li}_8\text{B}_8\text{H}_{32\text{--x}}\text{F}_x$ (1≤x≤4) thermodynamic properties, it can be a reasonable example among other possible partial H-atom substitution inside [BH,] $^-$ anion.
- (iii) RHCs based on LiBH₄ are a good idea because under changing of thermodynamics, the hydrogen storage capacity of the composite can be maintained.
- (iv) In spite of decreasing total hydrogen storage capacity for RHC mixtures with carbon nanofibers, the satisfied thermodynamic properties are retained. In addition, these carbon modifications might be discussed as catalytic effects on hydrogen sorption.

Taking into account the above-mentioned reaction enthalpy and hydrogen storage capacity Eqs. 12-25 only three reactions (17, 18 and 20) can be observed as promising ways for real LiBH $_4$ on-board applications. For better overall view, the graph with the total reaction enthalpy versus theoretical hydrogen content has been built in Fig. 5.

Interactions between ${\rm LiBH_4}$ and ${\rm LiNH_2}$, the RHC reaction between ${\rm LiBH_4}$ and ${\rm ScH_2}$, as well as carbon interaction with lithium borohydride (Eqs. 17, 18 and 20, correspondently) have the best compromise between thermodynamics and hydrogen gravimetric density. Therefore, they should be studied in detail and their challenges for other fuel cell requirements must be addressed as soon as possible.

3. Experimental results of LiBH₄ reversible decomposition

There are a lot of experimental results on LiBH $_4$ regarding its application in fuel cells, however, today there is no example which can be tested in practice. Indeed, some strong tendencies/certain approaches to describe and solve the problems are not so enlightened. In this chapter the main promising directions for LiBH $_4$ -based materials with working conditions in fuel cells have been collected.

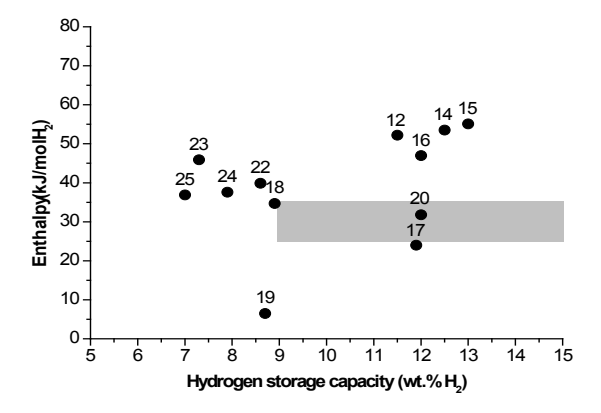


Figure 5. The reaction enthalpy (calculated by DFT without zeropoint energy correction [36]) at 300 K per 1 mol H₂ of (12-25) reactions versus theoretical hydrogen storage capacity. Gray rectangular squares describe fuel cell requirements.

3.1 Binary LiBH₄-LiNH₂ and ternary LiBH₄-LiNH₂-MgH₃ mixtures

The system of $LiBH_4$ – $LiNH_2$ in molar ratio 1:2 were studied experimentally in [37,38] and the reaction mechanism (Eq. 17) was confirmed by [44]. The quantities of desorbed hydrogen were experimentally deduced as approximately 7.9–9.5 wt.% H_2 . The decomposition reaction of $LiBH_4$ at approximately 800 K, while that of the mixture of $LiBH_4$ + $2LiNH_2$ proceeds at approximately 650 K. This indicates that the decomposition temperature of $LiBH_4$ reduces by 150 K because of mixing 2 mol of $LiNH_2$. The exothermic peak was observed at a slightly higher temperature of the hydride removal reaction of the mixture, but it could be due to the solidification of the product and not due to the exothermic hydride removal reaction of the mixture itself.

The two-step hydrogen absorption for Li_3N to form LiNH_2 + 2 LiH with theoretical hydrogen capacity ~10.4 wt.%H₂, was shown in [45]:

$$Li_3N + 2H_2 \rightarrow Li_2NH + LiH + H_2 \leftrightarrow LiNH_2 + 2LiH$$
 (26)

However, only the second reaction step can be reversible under practical conditions and releases around $\sim 5.2 \, \text{wt.} \% \, \text{H}_2$. By eliminating an extra LiH in this reversible reaction, the hydrogen storage capacity increases to $\sim 6.5 \, \text{wt.} \% \, \text{H}_2$:

$$LiNH_2 + LiH \leftrightarrow Li_2NH + 2H_2 \tag{27}$$

These reversible hydrogen reactions (Eqs. 26-27) were precursors before the detailed investigation of the LiBH₄–LiNH₂ system in [46,47]. A study of hydrogen and

ammonia release from the series of reactant mixtures (LiBH₄)_{1,2}(LiNH₂), was performed in [46]. It was found that maximum hydrogen and minimum ammonia release occur at x = 0.667 that corresponds to the composition LiB_{0.33}N_{0.67}H_{2.67}. In addition, a non-equilibrium phase diagram shows the occurrence of the various crystalline phases (α ; β ; γ ; δ with melting temperatures at 150–190; 75-90; ~45; ~50°C, respectively) and their correlation with released gases (H2 and NH3) was constructed. Experimental results confirmed that at ~250°C almost entirely hydrogen gas (~11.0 wt.% H₂ and ~1.6 wt.% NH₃) was desorbed from molten (LiBH₄)_{0.333}(LiNH₂)_{0.667} mixture. Improved hydrogen from the mixture was successfully proposed by incorporation of a small amount of noble metal (Pd; Pt) in [47]. For example, in samples of LiB_{0.33}N_{0.67}H_{2.67} with 0.29 mol% Pt (Pt/Vulcan carbon) the midpoint of hydrogen release was reduced by -90°C. Hydrogen release becomes detectable by mass spectrometry at temperatures ~115°C, and the onset of significant weight loss in Ar or He gas begins at ~150°C. The quantity of ammonia produced during dehydrogenation is substantially reduced. This appears to be a sizable temperature interval below ~210°C in which H₂ is released with little or no accompanying NH₃ production. Also, it was mentioned that the total quantity of NH3 released depends on how much of the dehydrogenation is conducted below NH₃-producing temperatures. Calorimetric results indicated that the dehydrogenation process is exothermic in both additivefree and additive-containing LiB_{0.33}N_{0.67}H_{2.67}. Therefore, rehydrogenation by pressurized hydrogen gas appears to be thermodynamically unfavorable. Only ~15% of the released hydrogen was recovered by 91 bar hydrogen pressure at relatively low temperatures. The authors of [47] give some assumption that there is no direct evidence for recovery of the α-phase, possibly because hydrogen absorption occurs through the formation of hydride species, such as LiH, LiNH, or Li, NH. The mechanism by which noble metals promote hydrogen release is speculative now. Calorimetric measurements also suggest that additives do not produce large changes in thermodynamics, supporting the view that improved hydrogen release arises predominantly from faster low-temperature kinetics. A similar kinetic effect was observed for Li, BN, H, by NiCl, in [48]. In the absence of the catalyst, this composition simultaneously releases H₂ and NH₃ in roughly equal quantities by weight at temperatures above 240°C. When Ni in the form of NiCl, is added as a dehydrogenation catalyst, only the H₂ release temperature is reduced by 122°C while NH₃ release still occurs at the higher temperature. This result clearly demonstrates that because of the catalyst two gases are evolved in two distinct decomposition reactions that are coincident in uncatalysed Li₄BN₃H₁₀. This is not a result of a single decomposition reaction but rather is two separate H₂ and NH₃ decompositions.

Additional examples of mixed complex hydrides together with binary metal hydride as appear to be a complicated ternary mixture [48-50] although they had shown quite good properties with the purpose of fuel cell applications. To enhance the properties of the above-mentioned binary mixtures, the ternary system LiBH,-LiNH,-MgH, was chosen in [48]. The choice of 1:2:1 stoichiometry was based on several factors: (1) the constituent hydrides and their binary mixtures all possess high gravimetric/volumetric capacities; (2) mixtures containing MgH, are known to suppress ammonia release from nitrogen-containing hydrides such as LiNH₂; (3) a stable lightweight compound (Li-Mg-B-N) known as a potential dehydrogenated product phase contains Mg, B, N in stoichiometry 1:1:2 as follows from the stoichiometric mixture. Experiments had shown that the unique desorption for the ternary mixture has a reaction mechanism that is not a simple superposition of the known binary mixtures:

$$3 \operatorname{LiNH}_{2} + \operatorname{LiBH}_{4} \to \operatorname{Li}_{4} \operatorname{BN}_{3} \operatorname{H}_{10} \tag{28}$$

$$Mg(NH_2)_2 + 2 LiH \leftrightarrow Li_2Mg(NH)_2 + 2 H_2$$
 (31)

$$\begin{array}{l} 3 \text{ Li}_{2} \text{Mg(NH)}_{2} + 2 \text{ LiBH}_{4} \rightarrow \\ & \rightarrow 2 \text{ Li}_{3} \text{BN}_{2} + \text{Mg}_{3} \text{N}_{2} + 2 \text{ LiH} + 6 \text{ H}_{2} \end{array} \tag{32}$$

$$\begin{aligned} \text{LiMgBN}_2(\text{unknown phase}) \rightarrow \\ \rightarrow \text{LiMgBN}_2(\text{Tetragonal}) \end{aligned} \tag{34}$$

$$2 \text{ LiH} \rightarrow \text{Li + H}_2 \tag{35}$$

Reactions by Eqs. 28-29 appear during ball milling during heating up to ~100 °C when $\mathrm{Li_4BN_3H_{10}}$ was molten. Further heating to 180 °C results in the release of ~2.0 wt.% $\mathrm{H_2}$ and corresponds to Eq. 30. In the temperature interval 180–225°C desorbed hydrogen increases to ~4.0 wt.% $\mathrm{H_2}$ by reaction (31). The next major hydrogen release occurs between 255–375°C that

corresponds to Eq. 32, thus in total ~8.2 wt.% H₂ was found. There is no hydrogen release in the temperature range 330-485°C, where an unknown phase was detected and two reactions could have place (see reactions (33-34)). And the last hydrogen desorption event was shown at 500-575°C by reaction (35). Through a wideranging experimental and first-principles computational analysis in [48] the self-catalyzing mechanism arose from a set of coupled ancillary reactions that yield both a homogenizing ionic liquid phase (Li,BN,H,0) and product nuclei for a subsequent reversible hydrogenstorage reaction (Mg(NH2)2/LiH system). These effects combine to yield enhanced low-temperature desorption kinetics and a significant reduction in ammonia liberation relative to the state of the art binary constituent mixtures. In order to establish the impact of the MgH_a in LiBH,-LiNH,-MgH, system the ternary mixture LiBH₄(LiNH₂)₂(MgH₂)₄ (0≤x≤1) had been studied in [49]. In conclusion, LiBH₄(LiNH₂)₂MgH₂ show the least ammonia release (<0.1 wt.% NH₃) and the largest value of hydrogen desorption (~4.0 wt.% H₂) at a lowtemperature event (~160°C).

The next promising example of a ternary mixture may be $LiBH_4$ – $Mg(NH_2)_2$ –LiH system. The mixtures of this with stoichiometry of 0.05:1:2; 0.1:1:2; 0.2:1:2 and 0.3:1:2 were thoroughly investigated in [50]. Kinetic and thermodynamic improvements in the hydrogen sorption properties of the binary $Mg(NH_2)_2$ –LiH system were achieved by introducing a small amount of $LiBH_4$. Hydrogen release at ~140°C and uptake at ~100°C was accelerated by a factor of two, while the temperature of equilibrium pressure at 1 bar decreased by 20°C to ~70°C. The in situ formed solid solution between $LiBH_4$ and $LiNH_2$ with weakened N–H bonds may be attributed to the enhancement of the hydrogen sorption kinetics.

In conclusion, a general characteristic of a LiBH₄–LiNH₂ system can be described by the general equation in a groundbreaking work [51]:

$$\frac{y}{x} M^{1}H_{x} + M^{2}(NH_{2})_{y} \rightarrow \frac{y}{x} M^{1}(NH)_{x/2} + H^{2}(NH)_{y/2} + H^{2}(NH)_{y/2}$$

where M¹ and M² are alkali or alkaline-earth metals. The main principle is interaction between negatively charged hydrogen [H]⁻ in ionic hydrides (e.g. in LiH, NaH) or partially negatively charged hydrogen [H]⁵⁻ in complex hydrides (e.g. in ([BH₄]⁻, [AlH₄]⁻) with partially positively charged hydrogen [H]⁵⁺ in covalent hydrides (e.g. in LiNH₂, NH₃, H₂S), so called "electron donor-acceptor" mechanism:

$$[H]^{\delta+} + [H]^{\delta-} \to 2 [H]^0 \to H_2$$
 (37)

This proposed reaction mechanism provides a reasonable explanation for destabilizing metal hydrides from an energy standpoint and can be applied as theoretical guidance for the screening of potential hydrogen storage materials.

3.2 LiBH $_4$ -MH $_2$ (M = Sc, Mg, Ce) as reactive hydride composites

Among $\mathrm{MH_2}$ (M = Sc, Ce, Mg,) scandium hydride may appear to be rather unpromising, since the experimentally observed reaction enthalpy for decomposition of $\mathrm{ScH_2}$, $\mathrm{CeH_2}$ and $\mathrm{MgH_2}$ was estimated to be ~258 [52]; ~193.3 [53] and ~76.1 [54] kJ $\mathrm{mol^{-1}}$ H₂, respectively. But this thermodynamically stable hydride ($\mathrm{ScH_2}$) can react with $\mathrm{LiBH_4}$ and exothermically produce $\mathrm{ScB_2}$ and LiH under ~1 bar equilibrium hydrogen pressure at 330 K (reaction (18)). $\mathrm{LiBH_4}$ – $\mathrm{ScH_2}$ system is one of the best promising examples of RHCs with regards to fuel cell applications, although it is not yet thoroughly studied.

In a contrast, the LiBH,-MgH, system is very well developed by Prof. John Vajo's group [55-58] and Prof. Rüdiger Bormann's groups [59-64] independently. In fact, the idea of RHC was proposed by latter group and verified mostly for 2LiBH,-MgB,. Indeed, magnesium hydride as a reactive additive enables simultaneously to retain hydrogen capacity and exothermically react with LiBH₄, produces new compound – MgB₂ (reaction (12)). Mechanically milled mixtures of LiBH, with MgH, with a 2:1 molar ratio are shown to store hydrogen above ~8 wt.% H₂ reversibly and extrapolation of isotherm predicted equilibrium hydrogen pressure of ~1 bar at approximately ~450 K. Individual decomposition of LiBH, and MgH, was observed at higher temperatures and low pressures (T ≥ 720 K and P ≤ 3 bar) whereas simultaneous desorption of H_a from LiBH, and formation of MgB₂ took place at T≈670 K and a hydrogen pressure around ~5 bar [64]. Strong influence of stoichiometry on the reaction pathway and cycling kinetics has been observed in [65]. That fact was associated with the initial reaction of deuterium at the surface of the sample, but the rate of the subsequent reaction was decreased because the high LiBD, content material may result in the encapsulation of MgD2 within the LiD matrix, hindering the mass transport required for further reaction.

In recent paper [66], the reaction pathway for interaction LiBH₄ with M (M = Mg, Ti, Sc) was proposed from a thermodynamic standpoint:

$$\begin{aligned} \text{LiBH}_4 + \frac{1}{2} \text{M} &\rightarrow \frac{3}{4} \text{LiBH}_4 + \frac{3}{8} \text{MH}_2 + \\ &+ \frac{1}{8} \text{MB}_2 + \frac{1}{4} \text{LiH} &\rightarrow \frac{1}{2} \text{MB}_2 + \text{LiH} + \frac{3}{2} \text{H}_2 \end{aligned} \tag{38}$$

But only in the case of Mg the reaction (38) with subsequent (12) were performed at 1 bar hydrogen pressure and temperatures 640-670 K that produced ~8.8 wt.% H₂ during 100 h [67]. It means that for Ti and Sc, reaction (38) is controlled by some kinetic barriers (possibly by the high melting temperature of M) and for them formation of new stable phases (MB₂ and LiH) is not simultaneous with LiBH₄ decomposition. Nevertheless, a kinetic effect on LiBH₄ decomposition by Ti and Sc (and other transition metals) were observed and resulted in lowering of T_d. It should be noted that the Mg reaction (38) is totally reversible and during cycling some kinetic improvements also take place.

In the case of the LiBH $_4$ –CeH $_2$ system, metallic Ce was used instead of cerium hydride, because of difficulties in obtaining CeH $_2$ [53]. Because of the total reaction enthalpy (27.6 kJ mol $^{-1}$ H $_2$) from a thermodynamic standpoint, reaction (39) seems to be possible:

$$LiBH_4 + \frac{1}{6}Ce \rightarrow LiH + \frac{1}{6}CeB_6 + \frac{3}{2}H_2$$
 (39)

However, exothermic reaction (40) with negative enthalpy value ($-193.3 \text{ kJ mol}^{-1} \text{ H}_2$) will happen when hydrogen is present:

$$Ce + H_2 \rightarrow CeH_2 \tag{40}$$

Thus, the two reactions, (39) and (40), give us the total process (41) with enthalpy value ($-135.7 \text{ kJ mol}^{-1} \text{ H}_2$):

$$\frac{6}{10}$$
LiBH₄ + Ce $\rightarrow \frac{6}{10}$ LiH + $\frac{9}{10}$ CeH₂ + $\frac{1}{10}$ CeB₆ (41)

Indeed after ball milling CeH₂ was detected by XRD analysis, and for the LiBH₄–CeH₂ system the reaction would be as follows:

$$LiBH_4 + \frac{1}{6}CeH_2 \rightarrow LiH + \frac{1}{6}CeB_6 + \frac{10}{6}H_2$$
 (42)

Theoretically, the reaction enthalpy for reaction (42) is 27.6 kJ mol $^{-1}$ H $_2$ and the maximal hydrogen capacity is ~7.3 wt.% H $_2$. RHCs of this system decomposed at temperatures close to melting point of pure LiBH $_4$, which is why at 446 K it is possible to reach ~1 bar equilibrium hydrogen pressure. In practice, LiBH $_4$ –CeH $_2$ system has better kinetic properties than LiBH $_4$ –MgH $_2$ and is fully reversible.

In conclusion, among of large number of possible RHCs theoretically and experimentally predicted in [68,69], the $\mathrm{MH_2}$ (M = Sc, Mg, Ce) can be promising destabilizing reagents for $\mathrm{LiBH_4}$ for the purpose of reversible hydrogen storage in fuel cells.

3.3 LiBH₄ nano-confinement by carbon framework

Since decomposition of LiBH₄ or its RHCs take place at temperatures above the melting point of LiBH, the reactive powder tends to be agglomerated or sintered. This behavior to enlarge particle size leads to slow kinetics in most cases. Therefore, an inert media with a special design would be helpful to prevent reagents from this negative effect by the confinement of the nanoparticles. The first approaches of this so called "nano-confinement" were observed in experiments involving MWCNTs and single-wall carbon nanotubes (SWCNTs) for MgH₂ [70], LiBH₄ [71] and their mixtures [72]. In all cases, these carbon modifications showed improvement in H-exchange kinetics. Today there are two explanations for the effect: (i) MWCNTs or SWCNTs may act as a milling aid (to increase the distribution of host material or even adsorb possible contaminates); (ii) they may form a net-like structure and exert nanoconfinement of the reactive powder. This new approach can be a very useful tool under hydrogen release/ uptake cycling where the entire composite would keep its unique nanostructure and thus keep a constant rate of hydrogen absorption/desorption.

The idea of nano-confinement was recently proposed by a carbon aerogel scaffold with pore size ~20 nm in [63]. The bottom-up approach where nanoparticles of hydrides are synthesized and infiltrated in nano-porous inert material demonstrated several advantages: (i) increased surface area of the reactants; (ii) nanoscale diffusion distances; (iii) increased number of grain boundaries, which facilitate reversible hydrogen sorption. DSC measurements for LiBH, -MgH, mixtures in a 2:1 molar ration showed that nano-confined samples released ~4.3 wt.% H₂ (100% from theoretical) while unmodified samples released ~9.2 wt.% H2 (only 80% from theoretical) at temperatures 530-740 K in Ar flow with 5/K rate heating. Moreover, a large shift to lower temperatures and another shape of hydrogen desorption peaks may indicate some improvement of both kinetics and thermodynamics. Unfortunately, XRD analysis performed in this experimental work did not provide an answer as to whether some new phases/intermediates were present as a result of carbon interaction with LiBH, (e.g. reactions (20-22)). Therefore, identification of the intermediates would be a proof of a thermodynamic effect in addition to kinetic improvements.

The same effects were observed in another experimental work [73] where a nano-confined sample was prepared by direct melt infiltration of bulk LiBH $_4$ – MgH $_2$ mixtures into the carbon aerogel. The modified

sample revealed a single step of dehydrogenation and a shift of about 50 K was detected in lower temperatures. The results of the work showed a more simple preparation of nano-confined RHCs and their improvement in H-exchange kinetics.

Obviously nano-confinement may diminish the negative effects of molten LiBH₄ under hydrogen desorption or reabsorption, thus maybe having an influence on the reaction mechanism of hydrogen absorption/desorption for LiBH₄ or its RHCs. Moreover, this new approach can be developed to become an important tool for nanotechnologies with improvements in the chemical reaction yields.

3.4 Effect of additives under LiBH₄ decomposition

The appearance of experimental evidence in kinetic improvement of reversible middle-temperature complex hydrides that are based on Na, Li and Al by titanium additives was the beginning of a new scientific direction made by Bogdanovic and Schwickardi [74]. Since that time a large amount of results about kinetic effects on hydrogen reactions of LiBH₄ or its RHCs have been produced. However, because of the high reactivity of LiBH₄, it is not so easy to find an example of a catalyst (additive which is not consumed by chemical reaction). In most cases, proposed additives behave as reagents that produce intermediates but finally cannot be recovered. A general catalytic mechanism for the reaction between LiBH₄ and MX_n additive (where M is metal with n valency; X is halogen) would be presented as follows:

$$n LiBH_4 + MX_n \rightarrow n LiX + M(BH_4)_n$$
 (43)

$$n LiX + M(BH4)n \rightarrow n LiX + MBn + 2n H2$$
 (44)

n LiX +
$$MB_n$$
 + 2n $H_2 \rightarrow MX_n$ + n LiH +
+ n B + 3n/2 H_2 (45)

Because of the higher temperature of crystallization compared to the temperatures used in [75], the presence of $Ti(BH_4)_3$ as a product of reaction (43) was not confirmed. However, a solid state reaction between LiBH $_4$ and $TiCl_3$ was observed at room temperature with LiCl formation. Moreover, firstly it was confirmed that solid LiCl can be dissolved in the structure of solid h-LiBH $_4$ at temperatures 373–518 K. A similar result was observed in [76] where XRD analysis with $TiCl_3$ always showed a LiBH $_4$ peak with very low intensity. In 1949, the reaction mechanism for the interaction between LiBH $_4$ and $TiCl_4$ was proposed in [77]:

$$\begin{array}{c} 4 \; {\rm LiBH_4} + {\rm TiCl_4} \rightarrow {\rm Ti(BH_4)_3} + \\ + 4 \; {\rm LiCl} + \frac{1}{2} \, {\rm B_2H_6} + \frac{1}{2} \, {\rm H_2} \end{array} \eqno(46)$$

It is concluded that the dehydrogenation temperature of $Ti(BH_4)_3$ was ~298 K. Thus, at room temperature and ambient pressure, $Ti(BH_4)_3$ decomposed by releasing hydrogen and a trace amount of gaseous B_2H_6 . Therefore, similar ion-exchange interactions (reaction (43)) could take place in case of LiBH₄ with MgCl₂ [78], MnCl₂ [79] or ZnF₂ [80].

In the case of HRCs based on LiBH, the additives react with LiBH, in a similar way [60,62], however, the attendant metal hydride (e.g. MgH, in reaction (12)) plays an additional role in the kinetic improvement [81-83]. For the LiBH₄-MgH₂-Ti{OCH(CH₃)₂}₄ mixture with a 2:1:0.1 molar ratio after ball milling TiO, anatase was found and during the first hydrogen desorption, Ti₂O₃ and TiB, appeared to be stable for further cycling [82]. XPS analysis showed that the reduction of titanium to Ti(III) was coupled to the migration of titanium species from the surface to the bulk of HRC. Two main factors, related to favoring heterogeneous nucleation of MgB and the increase of interfacial area trough grain refinement were proposed as the potential driving force for kinetic improvement. The influence of additives and microstructure refinement in the LiBH4-MgH2 system were studied in [83]. Transition metal borides (e.g. ZrB₂, ScB₂, VB₂, TiB₂) are characterized by the same hexagonal lattice structure as MgB, with a very small (0.1-3%) directional and interplanar misfit. This fact is a necessary condition for heterogeneous nucleation of MgB, because of the lowering of interfacial energy caused by transition metal borides or subsequently by additives. A good additive distribution and its sufficient amount were found as the main reason of the efficient heterogeneous nucleation of MgB₂. However, because of no change of the limiting rate neither for hydrogen absorption (contracting volume model) nor for desorption (interfaced-controlled one-dimensional growth), caused by the additives, the latter do not show catalyst behavior.

For some metals (Al and Cr) thermodynamically favorable chemical reactions between them and LiBH₄ were proposed as follows [67]:

$$2 \text{ LiBH}_4 + M \rightarrow MB_2 + 2 \text{ LiH} + 3 \text{ H}_2 \text{ (M = AI, Cr)}$$
 (47)

In experimental works [84,85] aluminum diboride was found to form and vanish during hydrogen release/uptake. This may be the first example of a catalyst for the reversible LiBH₄ decomposition where hydrogen dissociation to atoms and recombination to H₂ molecules was accelerated by aluminum at the hydride surface.

In recent work [86] mixtures of LiH–MgB₂–X (X = TiF_4 , TiO_2 , TiN, TiC) in a 2:1:0.1 molar ratio were studied as hydrogen storage material. Only TiF_4 had a chemical interaction with LiH similar to that which was found also for TiF_3 in [87]:

$$3 \text{ LiH} + \text{TiF}_3 \rightarrow 3 \text{ LiF} + \text{TiH}_2 + \frac{1}{2} \text{H}_2$$
 (48)

However for mixtures with TiO₂, TiN, and TiC additives, no new phase formation and clear signals for TiO₃, TiN, TiC, respectively, was detected by XRD. For comparison, an example of LiH-MgB2-TiO2(rutile) composite together with unmodified LiH-MgB, are presented in Figs. 6 and 7, respectively. About the same hydrogen storage capacity was achieved in LiH-MgB2-TiO2(rutile) and LiH-MgB₃, but the kinetics, especially for desorption, were drastically improved by rutile. It is expected that the behavior of TiO, as a catalyst may be similar to that as in the case of MgH2. In [88], it was concluded that uniform distributed rutile on the surface of MgH₂ could develop hydrogenation on the surface layer of Mg, which would increase the available path for hydrogen atoms by their fast diffusion into the bulk. In another experimental work [89] found that the anatase form

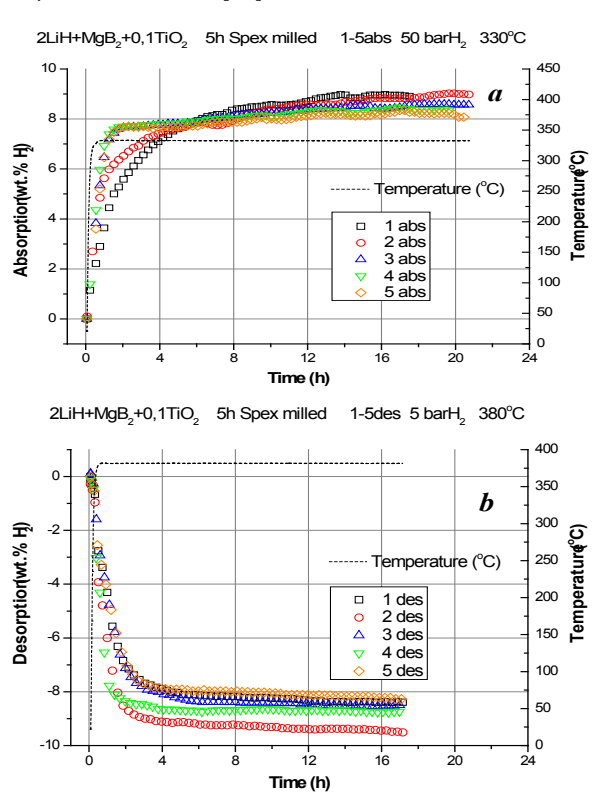


Figure 6. Hydrogen sorption for LiH-MgB₂-TiO₂(rutile) in a 2:1:0.1 molar ratio during 5 cycles. Absorption was performed at 330°C and 50 bar of hydrogen pressure (a); desorption was performed at 380°C and 5 bar H₂(b).

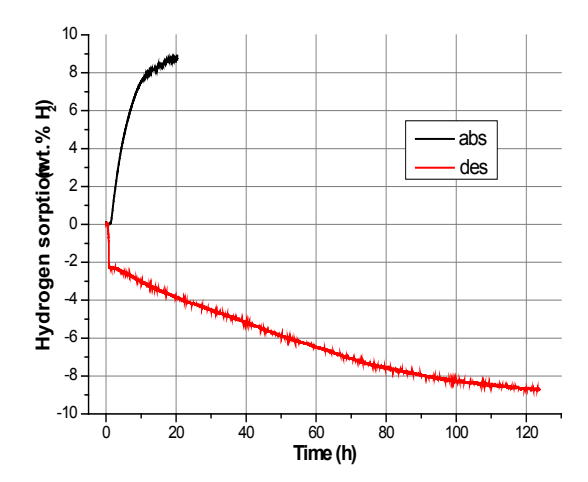


Figure 7. Hydrogen sorption for LiH-MgB₂ in a 2:1 molar ratio. Conditions for absorption and desorption were 350°C at 50 bar H₂ and 380°C at 5 bar H₂, respectively.

of TiO₂ is more effective than rutile because of higher surface areas which resulted in a better dispersion of active sites throughout MgH₂.

It should be mentioned that transition metal oxides are more promising additives for hydrogen uptake than pure transition metals although the latter have orders of magnitude higher activity to hydrogen [90-95]. Obviously, the explanation of catalytic effect by metal oxides should be found by tools of surface science. Indeed, the interaction of high surface area oxides (alumina, titania or their mixtures) with gas is concerned with heterogeneous catalysis. With respect to alumina or

titania, the single phase alumina-titania solid acids [96] have stronger acid sites and greater acid site density. These facts, coupled with their high surface area, produce the materials with an even greater number of acid sites per gram, making them useful heterogeneous catalysts.

4. Outlooks

Indeed LiBH₄ has potential to release/uptake hydrogen at moderate conditions and the sluggish kinetics are considered to be primarily responsible for the high reaction temperature [97]. Therefore, practical strategies to achieve fast reaction kinetics will be the most important scientific direction for the purpose of applications of LiBH₄ in fuel cells. Thus, hydrogen fuelled vehicles will be able to match the performance of that of a hydrocarbon car at comparable cost (around US\$5 (kW h)⁻¹ [2]).

Acknowledgments

The author wishes to thank Drs. Martin Dornheim, Ulrike Bösenberg, Klaus Taube and José Bellosta von Colbe (Helmholtz-Zentrum Geesthacht) for useful discussions. This work was supported by the European Commission (contract MRTN-CT-2006-035366).

References

- [1] L. Schlapbach, A. Züttel, Nature 414, 353 (2001)
- [2] D.K. Ross, Vacuum 80, 1084 (2006)
- [3] A. Züttel, S. Rentsch, P. Fesher, P. Wenger, P. Sudan, Ph. Mauron, Ch. Emmenegger, J. Alloy Comp. 356-367, 515 (2003)
- [4] Yu. Nakamori, S. Orimo, J. Alloy Comp. 370, 271 (2004)
- [5] M.S. Smith, G.E. Bass, J. Chem. Eng. Data 8, 341 (1963)
- [6] N. Ohba, K. Miwa, M. Aoki, T. Noritake, S. Towata, Yu. Nakamori, S. Orimo, A. Züttel, Phys. Rev. B 74, 075110 (2006)
- [7] H. Deiseroth, O. Sommer, H. Binder, K. Wolfer, B. Frei, Z. Anorg. Allg. Chem. 571, 21 (1989)
- [8] I. Kuznetsov, D. Vinitskii, K. Solntsev, N. Kuznetsov, L. Butman, Russ. J. Inorg. Chem. 32, 1803 (1987)
- [9] I. Tiritiris, T. Schleid, Z. Anorg. Allg. Chem. 629, 1390 (2003)
- [10] K. Miwa, N. Ohba, S. Towata, Yu. Nakamori, S. Orimo, Phys. Rev. B 69, 245120 (2004)
- [11] M. Smith, G. Bass, J. Chem. Eng. Data 8, 342

- (1963)
- [12] E. Jeon, Y. Cho, J. Alloy and Comp. 422, 273 (2006)
- [13] A. Züttel, A. Borgschulte, S. Orimo, Scr. Mater. 56, 823 (2007)
- [14] L. Mosegaard, B. Møller, J.-E. Jørgensen, U. Bösenberg, M. Dornheim, J.C. Hanson, Y. Cerenius, G. Walker, H.J. Jakobsen, F. Besenbacher, T.R. Jensen, J. Alloys Comp. 446– 447, 301 (2007)
- [15] Ph. Mauron, F. Buchter, O. Friedrichs, A. Remhof, M. Bielmann, Ch. Zwicky, A. Züttel, J. Phys. Chem. B. 112, 906 (2008)
- [16] J. Nakamori, Sh. Orimo, J. Alloys Comp. 370, 271 (2004)
- [17] Y. Filinchuk, D. Chernyshov, V. Dmitriev, Z. Kristallogr. 223, 649 (2008)
- [18] Y. Nakamori, K. Miwa, A. Ninomiya, H. Li, N. Ohba, S. Towata, A. Züttel, S. Orimo Physical Review B 74, 045126 (2006)
- [19] X.B. Xiao, W.Y. Yu, B. Yu. Tang, J. Phys.: Condens.

- Matter. 20, 445210 (2008)
- [20] E.A. Nickels, M.O. Jones, W.I.F. David, S.R. Johnson, R.L. Lowton, M. Sommariva, P.P. Edwards, Angew. Chem. 47, 2817 (2008)
- [21] X.-B. Xiao, W.-Y. Yu, B.-Y. Tang, J. Phys.: Con. Matter 20, 445210 (2008)
- [22] H. Hagemann, M. Longhini, J.W. Kaminski, T.A. Wesolowski, R. Cerny, N. Penin, M.H. Sørby, B.C. Hauback, G. Severa, C.M. Jensen, J. Phys. Chem. A 112, 7551 (2008)
- [23] J.S. Hummelshøj, D.D. Landis, J. Voss et al., J. Chemical Physics 131, 014101 (2009)
- [24] A. Bouamrane, J.P. Laval, J.P. Soulie, J.P. Bastide, Materials Research Bulletin 35, 545 (2000)
- [25] N. Eigen, U. Bösenberg, J. Bellosta von Collbe, T.R. Jensen, Y. Cerenius, M. Dornheim, T. Klassen, R. Bormann, J. Alloys Comp. 477, 76 (2009)
- [26] A. Bouamrane, C. Brauer, J.P. Soulie, J.M. Letoffe, J.P. Bastide, Thermochimica Acta 326, 37 (1999)
- [27] L. Yin, P. Wang, Zh. Fang, H. Cheng, Chemical Physics Letters 450, 318 (2008)
- [28] J. Ph. Soulie, G. Renaudin, R. Cerny, K. Yvon, J. Alloys Comp. 346, 200 (2002)
- [29] M. Corno, E. Pinatel, P. Ugliengo, M. Baricco J. Alloys Comp., DOI:10.1016/j.jallcom. 2010.10.005
- [30] I. Saldan, R. Gosalawit-Utke, C. Pistidda,
 U. Bösenberg, J.M. Ramallo-López, F.G. Requejo,
 M. Schulze, T. Klassen, K. Suarez-Alcantara,
 J. Bellosta von Colbe, K. Taube, M. Dornheim,
 J. Phys. Chem. C (in press)
- [31] R. Gosalawit, J.M. Bellosta von Colbe, M. Dornheim, T.R. Jensen, Y. Cerenius, Ch.M. Bonatto, M. Peschke, R. Bormann, J. Phys. Chem. C, 114, 10291 (2010)
- [32] T. Ruman, A. Kusnierz, A. Jurkiewicz, A. Les, W. Rode, Inorg. Chem. Comm. 10, 1074 (2007)
- [33] J.G. Gainsford, T. Kemmitt, G.B. Jameson, S.G. Telfer, Acta Cryst. C. 65, 180 (2009)
- [34] Z. Xiong, C.K. Yong, G. Wu, P. Chen, W. Shaw, A. Karkamkar, T. Autrey, M.O. Jones, S.R. Johnson, P.P. Edwards, W.I.F. David, Nature Mat. 7, 138 (2007)
- [35] J. Vajo, S. Skeith, F. Mertens, J. Phys. Chem. B 109, 3719 (2005)
- [36] S. Alapati, J. Johnson, D. Sholl, Phys. Chem. Chem. Phys. 9, 1438 (2007)
- [37] F. Pinkerton, G. Meisner, M. Meyer, M. Balogh, M, Kundrat, J. Phys. Chem. B 109, 6 (2005)
- [38] M. Aoki, K. Miwa, T. Noritake, G. Kitahara, Y. Nakamori, S. Orimo, S. Towata, Appl. Phys. A. 80, 1409 (2005)
- [39] Y. Filinchuk, K. Yvon, G. Meisner, M. Meyer, F. Pinkerton, M. Balogh, Inorg. Chem. 45, 1433

- (2006)
- [40] N. Jacobson, B. Tegner, E. Schroder, P. Hyldgaard, B. Lundqvist, Comput. Mater. Sci. 24, 273 (2002)
- [41] Z. Zhu, G. Lu, S. Smith, Carbon 42, 2509 (2004)
- [42] F. Pinkerton, B. Wicke, C. Olk, G. Tibbetts, G. Meisner, M. Meyer, J. Herbst, J. Phys. Chem. B 104, 9460 (2000)
- [43] X. Yu, Z. Wu, Q. Chen, Z. Li, B. Weng, T. Huang, Appl. Phys. Lett. 90, 034106 (2007)
- [44] Y. Nakamori, A. Ninomiya, G. Kitahara, M. Aoki, T. Noritake, K. Miwa, Y. Kojima, S. Orimo, J. Pow. Sour 155, 447 (2006)
- [45] P. Chen, Z. Xiong, J. Luo, J. Lin, K. L. Tan, Nature 420, 302 (2002)
- [46] G. Meisner, M. Scullin, M. Balogh, F. Pinkerton, M. Meyer, J. Phys. Chem. B 110, 4186 (2006)
- [47] F. Pinkerton, M. Meyer, G. Meisner, M. Balogh, J. Phys. Chem. B 110, 7967 (2006)
- [48] J. Yang, A. Sudik, D.J. Siegel, D. Halliday, A. Drews, R.O. Carter, III, Ch. Wolverton, G.J. Lewis, J.W. Adriaan Sachtler, J.J. Low, S.A. Faheem, D.A. Lesch, V. Ozolinš, Angew. Chem. 47, 882 (2008)
- [49] A. Sudik, J. Yang, D. Halliday, A. Drews, Ch. Wolverton, J. Phys. Chem. C 112, 4384 (2008)
- [50] J. Hu, Y. Liu, G. Wu, Zh. Xiong, Y.Sh. Chua, P. Chen, Chem. Mater. 20, 4398 (2008)
- [51] J. Lu, Zh. Z. Fang, H.Y. Sohn, Inorg. Chem. 45, 8749 (2006)
- [52] S.V. Alapati, J.K. Johnson, D.S. Sholl, J. Alloys Comp. 446–447, 23 (2007)
- [53] S.-Ah Jin, Y.-S. Lee, J.-H. Shim, Y.W. Cho, J. Phys. Chem. C 112, 9520 (2008)
- [54] M. Pozzo, D. Alfè, Phys. Rev. B 77, 104103 (2008)
- [55] J. Vajo, S. Skeith, F. Mertens, J. Phys. Chem. B 109, 3719 (2005)
- [56] J. Vajo, G.L. Olson, Scr. Materialia 56, 829 (2007)
- [57] J. Vajo, T.T. Salguero, A.F. Gross, S.L. Skeith, G.L. Olson, J. Alloys Comp. 446–447, 409 (2007)
- [58] J. Vajo, Cur. Opin. Sol. St. Mater. Sci., DOI:10.1016/j. cossms.2010.11.001
- [59] G. Barkhordarian, T. Klassen, M. Dornheim,R. Bormann, J. Alloys Comp. 440, L18 (2007)
- [60] Y.-P. Zhou, MSc thesis, Helmholtz Zentrum Geesthacht (Geesthacht, Germany, 2007)
- [61] U. Bösenberg, S. Doppiu, L. Mosegaard, G. Barkhordarian, N. Eigen, A. Borgschulte, T.R. Jensen, Y. Cerenius, O. Gutfleisch, T. Klassen, M. Dornheim, R. Bormann, Acta Mater. 55, 3951 (2007)
- [62] U. Bösenberg, PhD thesis, Helmholtz Zentrum Geesthacht (Geesthacht, Germany, 2009)

- [63] T.K. Nielsen, U. Bösenberg, R. Gosalawit, M. Dornheim, Y. Cerenius, F. Besenbacher, T.R. Jensen, ACS Nano 4, 3903 (2010)
- [64] U. Bösenberg, D.B. Ravnsbæk, H. Hagemman, V. D'Anna, Ch. Bonatto Minella, C. Pistidda, Wouter van Beek, T.R. Jensen, Y. Cerenius, O. Gutfleisch, R. Bormann, M. Dornheim, J. Phys. Chem. C (in press)
- [65] T.E.C. Price, D.M. Grant, V. Legrand, G.S. Walker, J. Hydrogen Energy 35, 4154 (2010)
- [66] D.J. Siegel, Ch. Wolverton, V. Ozolinš, Phys. RevB: Con. Matter, Mater. Phys. 76, 134102 (2007)
- [67] J. Yang, A. Sudik, Ch. Wolverton, J. Phys. Chem. C 111, 19134 (2007)
- [68] S.V. Alapati, J.K. Johnson, D.S. Sholl, J. Phys. Chem. B, 110, 8769 (2006)
- [69] S.V. Alapati, J.K. Johnson, D.S. Sholl, J. Phys. Chem. C, 112, 5258 (2008)
- [70] C.Z. Wu, P. Wang, H.M. Cheng, J. Phys. Chem. B 109, 22217 (2005)
- [71] Z.Z. Fang, X.D. Kang, H.B. Dai, M.G. Zhang, P. Wang, H.M. Cheng, Scr. Mater. 58, 922 (2008)
- [72] P.-J. Wang, P.Z.Z. Fang, L.-P. Ma, X.-D. Kang, P. Wang, J. Hydrogen Energy 33, 5611 (2008)
- [73] R. Gosalawit-Utke, T. Nielsen, I. Saldan, Y. Cerenius, T.R. Jensen, T. Klassen, M. Dornheim, J. Phys. Chem. C (in press)
- [74] B. Bogdanovic, M. Schwickardi, J. Alloys Comp. 253-254, 1 (1997)
- [75] L. Mosegaard, B. Møller, J.-E. Jørgensen, Ya. Filinchuk, Y. Cerenius, J. Hanson, E. Dimasi, F. Besenbacher, T.R. Jensen, J. Phys. Chem. C, 112, 1299 (2008)
- [76] M. Au, A. Jurgensen, J. Phys. Chem. B 110, 7062 (2006)
- [77] H. Hoekstra, J. Katz, J. Am. Chem. Soc. 71, 2488 (1949)
- [78] M. Au, A. Jurgensen, K. Zeigler, J. Phys. Chem. B 110, 26482 (2006)
- [79] R.A Varin, L. Zbroniec, J. Hydrogen Energy 35, 3588 (2010)
- [80] M. Au, R.T. Walters, J. Hydrogen Energy 35, 10311 (2010)
- [81] U. Bösenberg, U. Vainio, P. Pranzas, J. Belosta von Colbe, G. Goerigk, E. Welter, M. Dornheim, A. Schreyer, R. Bormann, Nanothech. 20, 204003 (2009)

- [82] E. Deprez, M.A. Munoz-Marquez, M.A. Roldan, C. Prestipino, F.J. Palomares, Ch. Bonatto-Minella, U. Bösenberg, M. Dornheim, R. Bormann, A. Fernandez, J. Phys. Chem. C 114, 3309 (2010)
- [83] U. Bösenberg, J.W. Kim, D. Gosslar, N. Eigen, T.R. Jensen, J. Belosta von Colbe, Y. Zhou, M. Damhs, D.H. Kim, R. Günther, Y.W. Cho, K.H. Oh, T. Klassen, R. Bormann, M. Dornheim, Acta Mater. 58, 3381 (2010)
- [84] S.-A. Jin, J.-H. Shim, Y.W. Cho, K.-W. Yi, O. Zabara, M. Fichtner, Scr. Mater. 58, 963 (2008)
- [85] D. Blanchard, Q. Shi, B. Boothroyd, T. Vegge, J. Phys. Chem. C 113, 14059 (2009)
- [86] I. Saldan, R. Campesi, O. Zavorotynska, G. Spoto, M. Baricco, U. Bösenberg, A. Arendarska, K. Taube, M. Dornheim, J. Hydrogen Energy (in press)
- [87] P. Wang, L. Ma, Z. Fang, X. Kang, P. Wang, Energy Environ. Sci. 2, 120 (2009)
- [88] K.S. Jung, D.H. Kim, E.Y. Lee, K.S. Lee, Catalysis Today 120, 270 (2007)
- [89] D.L. Croston, D.M. Grant, G.S. Walker, J. Alloys Comp. 492, 251 (2010)
- [90] V.E. Henrich, P.A. Cox, The surface science of Metal Oxides, 2nd edition (Cambridge University Press, New York, 1994)
- [91] R. Hummer, J.K. Norskov, Sur. Sci. 343, 211 (1995)
- [92] R. Hummer, J.K. Norskov, Nature 376, 238 (1995)
- [93] G. Barkhordarian, T. Klassen, R. Borman J. Alloys Comp. 364, 242 (2004)
- [94] G. Barkhordarian, T. Klassen, R. Borman J. Phys. Chem. B 110, 11020 (2006)
- [95] A. Borgschulte, U. Bösenberg, G. Barkhordarian, M. Dornheim, R. Borman, Catalysis Today 120, 262 (2007)
- [96] G.S. Walker, E. Williams, A.K. Bhattacharya, J. Mater. Sci. 32, 5583 (1997)
- [97] H.-W. Li, Y. Yan, S. Orimo, A. Züttel, C.M. Jensen, Energies 4, 185 (2011)